QUANTUM DOTS

I

Janusz Adamowski

Faculty of Physics and Applied Computer Science
AGH University of Science and Technology, Kraków

2010/2011

Dziękuję Pani Joannie Tomkowicz za pomoc
w opracowaniu internetowej wersji wykładów.

Outline of Lectures

(1) Semiconductor nanostructures

(2) Self-assembled quantum dots

(3) Electrostatic quantum dots

(4) Single-electron tunnelling spectroscopy

(5) Poisson-Schrődinger problem

(6) Quantum Coulomb blockade

(7) Model confinement potentials

(8) Magnetic field effects

(9) Wigner molecules

(10) Fundamentals of quantum computation

(11) Quantum logic gates on quantum dots

1 Semiconductor Nanostructures

Structures fabricated from semiconducting materials with at least one spatial dimension limited to the interval

from ~ 1 to ~ 100 nm.

1.1 Classification of semiconductor nanostructures

(1) quasi-2D structures

- **(a)** single quantum well (QW) ($n = 1$)
- **(b)** multiple quantum wells (MQW) ($n = 2, \ldots, \sim 10$)
- **(c)** superlattice (SL) ($n \geq 10$)

(2) quasi-1D structures: quantum wires, nanowires

(3) quantum dots (QD)

- **(a)** nanocrystals
- **(b)** QD's in porous materials
- **(c)** self-organized QD's
- **(d)** electrostatic QD's

1.2 Fundamental property of QD's

Physical properties of QD's are strongly dependent on **size** of nanostructure.

Moreover, the physical properties of QD's are dependent on:

- geometric structure (in particular, shape)
- chemical composition
- external electric fields
- magnetic field
- strain at heterojunctions

Application of suitable technology and external fields (electric and magnetic) provides an opportunity of tuning the electronic properties of QD's in a **designed manner**.

$\Longrightarrow$ **quantum engineering**

2 Self-organized QD's (self-assembled QD's)

The self-organized QD's grow according to the **Stranski-Krastanov mechanism**:

- molecular beam of material A is deposited on the substrate from material B
- in the first stage, **the wetting layer** of material A is formed on substrate B
- in the next stages, the strain between materials A and B, which results from the misfit of lattice constants between A and B crystals, leads to a desegregation of the next doses of deposited material A
- this leads to the formation of islands consisting of material A on the wetting layer
- the islands possess nearly the same shapes and sizes, and moreover form an ordered structure on the substrate
  $\Longrightarrow$ **self-organization, self-assembly**
- as a result, we obtain a QD array, i.e., an array composed of many QD's with similar shapes, sizes, and interdot distances

Digression:

Polish explanation of prefix **nano**

deposition = nanoszenie (in Polish)

$\Longrightarrow$ **nanotechnology, nanostructure, ...**

Typical shapes of self-organized QD's:

stack, pillar, cone, truncated cone, pyramid, lens, cathedral, etc.

Typical sizes: height $\simeq$ 10 nm, base $\simeq$ 100 nm

Application of self-organized QD's:

semiconductor lasers (microlasers)

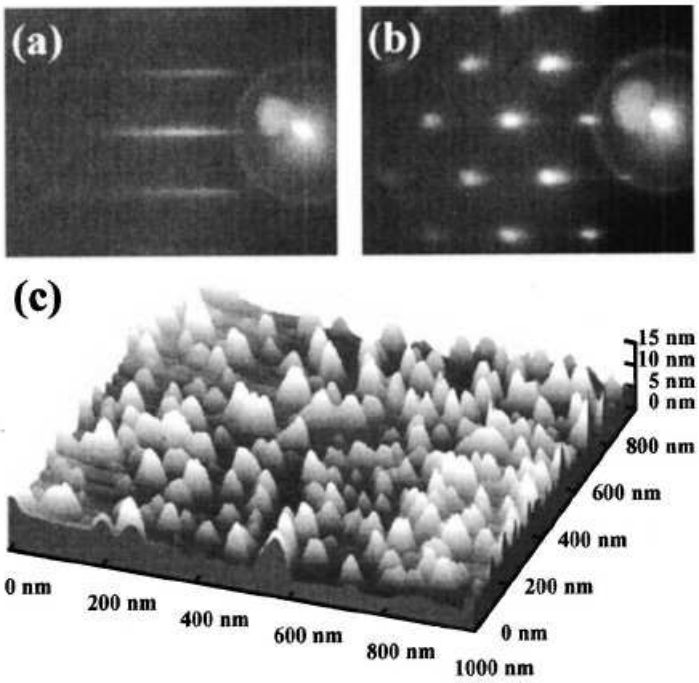

FIG. 1. 4.5 ML CdTe grown by MBE on ZnTe: (a) 2D RHEED pattern just after growth (i.e., before depositing amorphous Te), (b) 3D RHEED pattern after Te desorption, and (c) corresponding surface by UHV-AFM.

Figure 1: Self-organized CdTe QD's on ZnTe substrate.

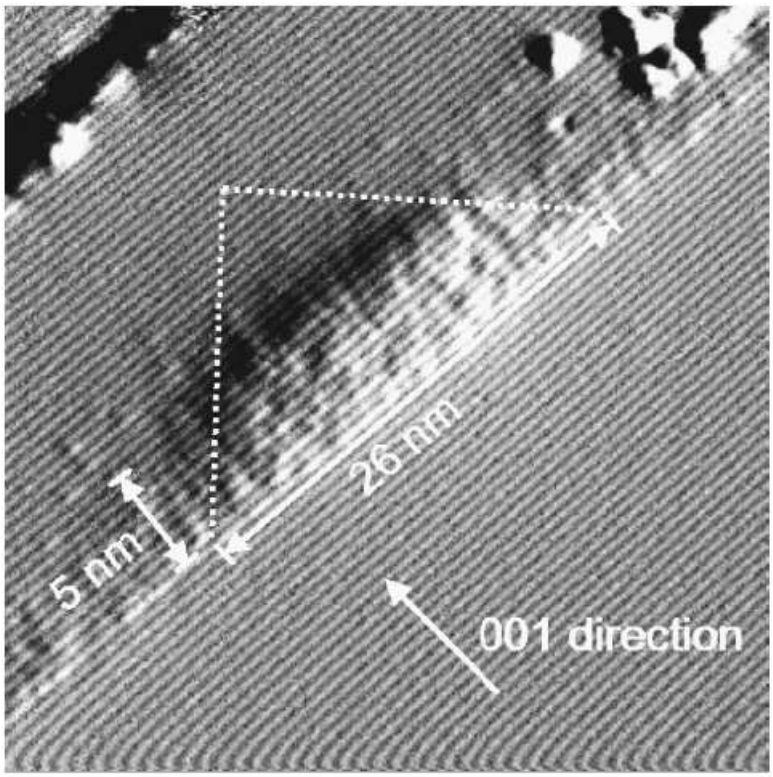

FIG. 1. $40 \times 40\ \mathrm{nm}^2$ X-STM current image of a cleaved InAs quantum dot and the wetting layer. In the upper right corner some cleavage debris is visible.

Figure 2: InAs QD on wetting layer.

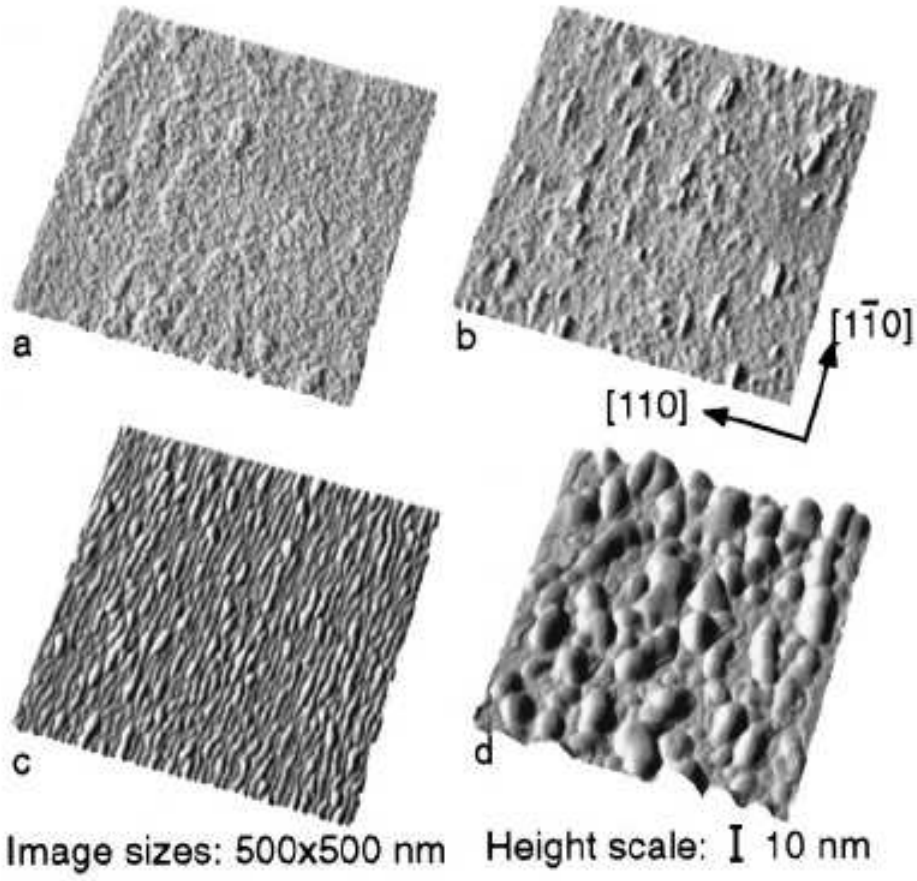

FIG. 1. AFM micrographs for different GaAs deposition amounts. (a) Epitaxial GaP surface (0 ML of GaAs). (b) 0.84 GaAs monolayers showing small elongated islands. (c) Corrugated surface after 5.0 GaAs monolayers. (d) Irregularly shaped islands after 10 GaAs monolayers.

Figure 3: Formation of GaAs islands on GaP substrate.

3 Electrostatic QD's

Called as well:

- Electrically defined QD's
- gate-defined QD's
- gate-controlled QD's, gated QD's

Basic reference:

J. Adamowski, S. Bednarek, B. Szafran
"Modeling of Electrostatically Gated Vertical Quantum Dots"
Handbook of Semiconductor Nanostructures and Nanodevices
Edited by A. A. Balandin and K. L. Wang
(American Scientific Publishers, 2006), Vol. 1, Chapter 9, pages 389-452

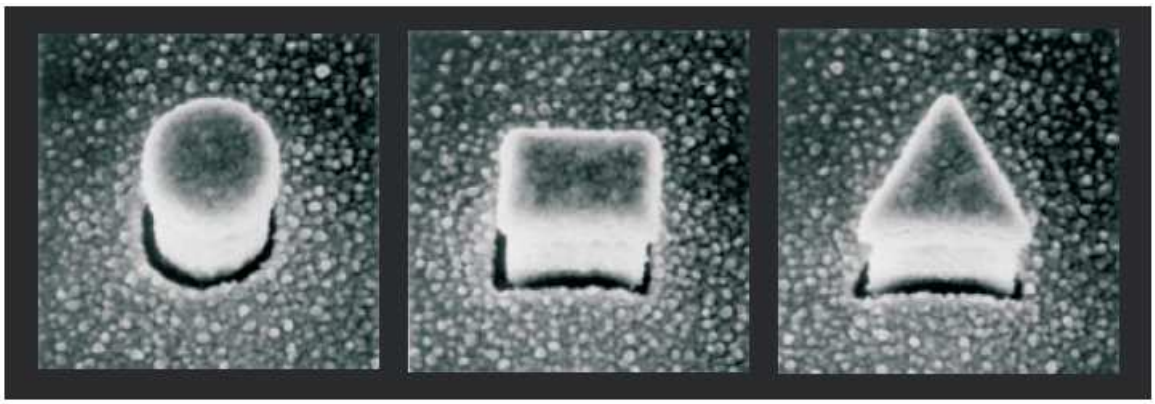

Figure 4: SEM photos of electrostatic QD's fabricated in the laboratory of Professor Seigo Tarucha, NTT, Japan. Width of pillars $\simeq 500$ nm.

3.1 Semiconductor nanodevices consisting of electrostatic QD's

Geometry of semiconductor nanodevices

- vertical (vertical QD's)
- lateral (lateral QD's)
- mixed (laterally coupled vertical QD's)

(a) two-terminal (two-electrode) nanodevices

(b) three-treminal (three-electrode) nanodevices

(c) many-terminal (many-electrode) nanodevices
(number of electrodes $= 4, 5, \ldots$**)**

3.2 Multiple QD's

- single QD (**artificial atom**)
- multiple QD's = coupled QD's (**artificial molecules**)
  - double QD's
  - triple QD's
  - quadruple QD's
  - ...
  - QD array (artificial crystal)

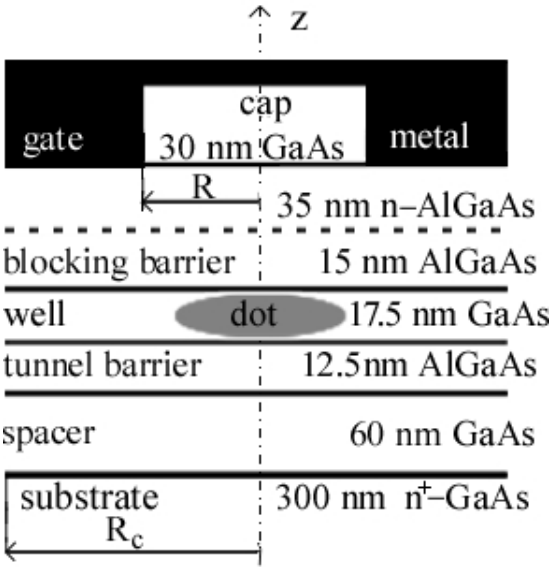

Figure 5: Schematic of two-electrode nanosystem [R.C. Ashoori et al., MIT)]. R = radius of GaAs cap, covered by a metal, R_c = radius of cylindrical surface, on which we put on the boundary conditions for the Poisson equation.

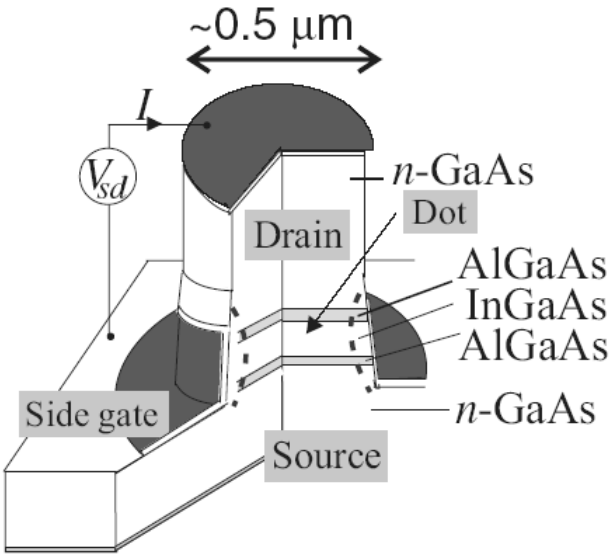

Figure 6: Schematic of vertical three-terminal nanosystem [S. Tarucha et al., NTT)].

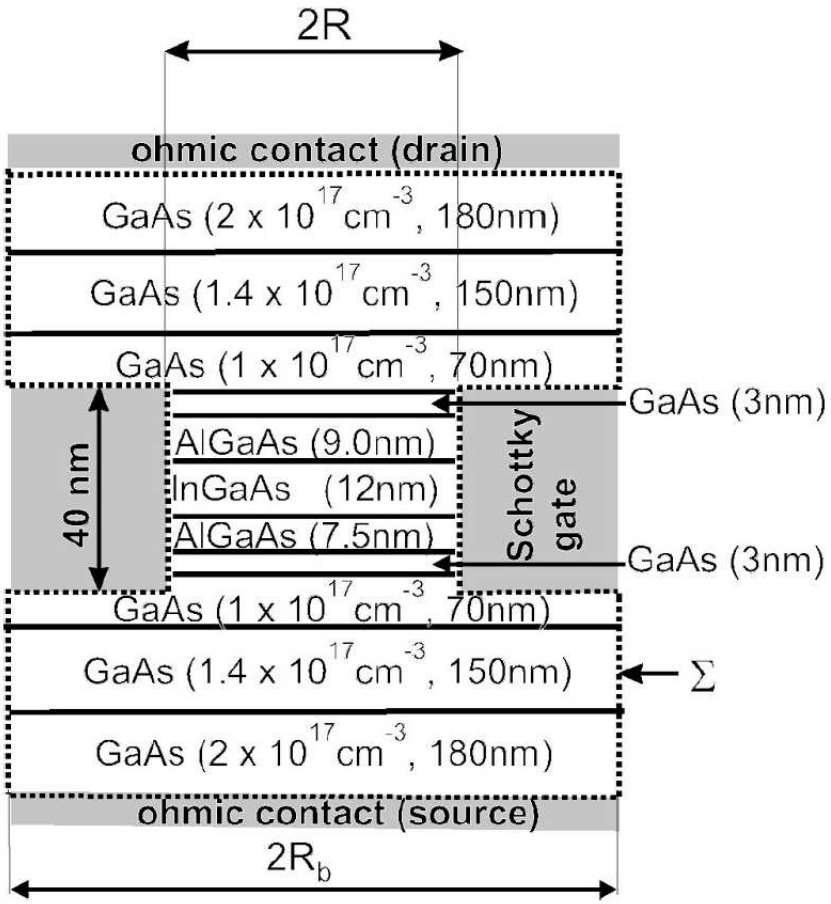

Figure 7: Schematic of vertical three-terminal nanosystem (Tarucha, NTT). Given are the donor concentrations and layer thicknesses.

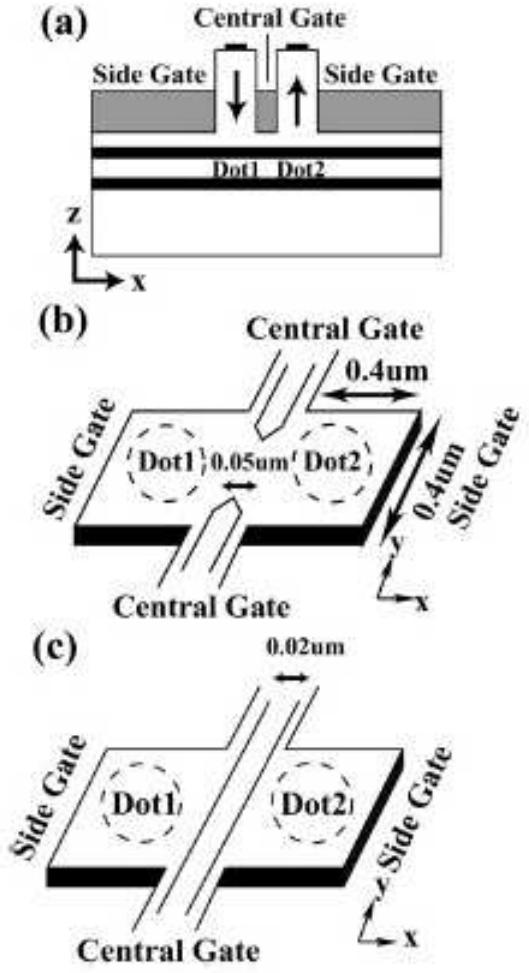

Fig. 1. (a) Cross-sectional view of the LCVQD system. The arrows indicate the direction of the current flow for charging the dots. (b) Top view of the split-gate LCVQD. The side gates surround the two dots providing confinement. The two central gates, which act as barriers between Dot1 and Dot2 are disconnected from one another. (c) Top view of the single-gate LCVQD. Unlike the split-gate, there is just a single, central gate cutting across the middle of the structure.

Figure 8: Schematic of laterally coupled vertical QD's [T. Hatano et al., (2005)].

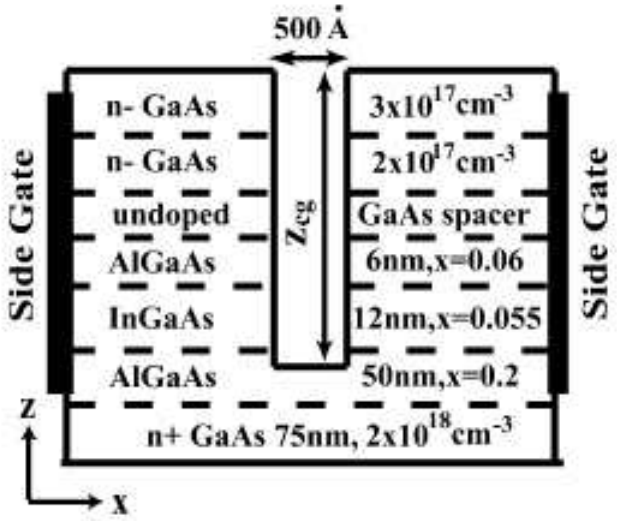

Fig. 2. (a) Schematic of the split-gate LCVQD system showing all the layers. The depth of the central gate is denoted by z_{cg}. The "dot" region is located in the InGaAs layer, between the two AlGaAs layers. (b) Schematic of the single-gate LCVQD system.

Figure 9: Cross section of layers in laterally coupled vertical QD's [T. Hatano et al., (2005)].

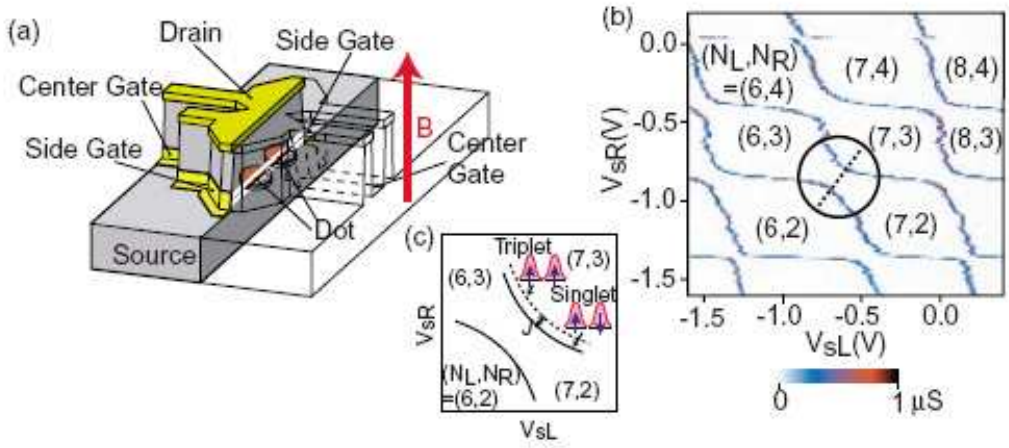

FIG. 1. (Color online) (a) Structure of DQD device. The red (dark gray) arrow shows the direction of the applied magnetic field. (b) Color plot of the conductance as a function of the left and right side gate voltages, V_{sL} and V_{sR}. (N_L,N_R) denote the electron number on the left and right QDs. The effective two-electron ground state is a singlet state and the excited state is a triplet state as shown schematically in (c).

Figure 10: Laterally coupled vertical QD's [T. Hatano et al., (2005)].

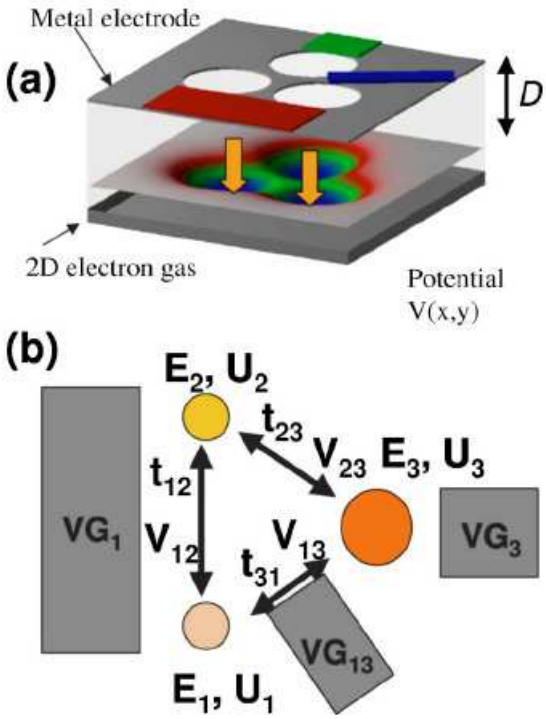

FIG. 1. (Color online) (a) Cross-sectional view of a model of the three coupled gated lateral quantum dots. The grey rectangular gate contains three circular openings, which translate into minima of the electrostatic potential at the level of the two-dimensional electron gas. The red and green gates can be used to shift the potential minima of the dots underneath them with respect to the rest of the system. The blue gate is used to tune the tunneling barrier between dots 1 and 3. (b) Schematic representation of the triple dot structure.

Figure 11: Triple laterally coupled QD's [M. Korkusinski et al., (2007)].

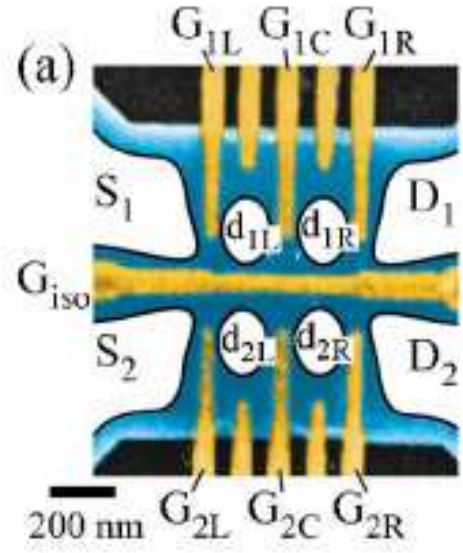

Figure 12: Quadruple laterally coupled QD's [G. Shinkai et al., (2007)].

4 Single-electron tunnelling spectroscopy

Excess electrons confined in a QD form spatially localized bound states (quasi-bound states) with discrete energy levels. $\Longrightarrow$ artificial atom states

Typical energy separations between discrete energy levels:

$$\Delta E_{mn} \simeq 1 - 10 \text{ meV}$$

4.1 Electrochemical potential

For a system of N electrons localized (or delocalized) in an arbitrary system **the chemical potential** is defined as the energy needed to increase the number of electrons by one, i.e.,

$$\mu_{N+1}^0 = E_{N+1} - E_N \ , \tag{1}$$

E_N = ground-state energy of N electron system

Chemical potential of electrode α

$$\mu_\alpha = \mu_\alpha^0 - eV_\alpha \ , \tag{2}$$

μ_α^0 = chemical potential of electrons in electrode α
V_α = voltage applied to electrode α
e = elementary charge ($e > 0$), this means that electron charge $q_e = -e$,

$\Longrightarrow -eV_\alpha = U_\alpha^e$ = potential energy of electron in electrode α

For a metal at temperature $T = 0$ and at $V_\alpha = 0$

$$\mu_\alpha = F_\alpha \ , \tag{3}$$

where F_α = Fermi energy

For a non-degenerate n-type semiconductor at $T = 0$

$$F_\alpha = E_D = \text{donor energy level}$$

For a degenerate n-type semiconductor

$$F_\alpha > E_c^{min} = \text{minimum energy of conduction band}$$

4.2 Conditions of single electron tunnelling

Tunnelling of a single electron from electrode α to the QD with N confined electrons is energetically allowed if

$$\mu_\alpha \geq \mu_{N+1} \ . \tag{4}$$

Inequality (4) determines **a condition of charging the QD by the single $(N+1)$th electron**.

If the inequality (4) is opposite, the electrons can tunel from the QD to electrode α.

$\Longrightarrow$ **capacitance spectroscopy**

4.3 Transport spectroscopy

We extend condition (4) to the case of single electron tunnelling from the first electrode (source, emiter) to the second electrode (drain, collector) through the QD

$$\mu_s \geq \mu_{N+1} \geq \mu_d \ , \tag{5}$$

μ_s (μ_d) = electrochemical potential of source (drain)

The electrochemical potentials of the source and drain depend on voltages applied to the source (V_s) and drain (V_d) electrodes [according to (2)].

If the Fermi energies of the source and drain are equal to each other, i.e., $F_s = F_d = F$, tunnelling condition (5) is determined by the source-drain voltage (bias voltage)

$$V_{sd} = V_s - V_d \equiv V_{bias} \ .$$

Tunnelling condition ("transport window")

$$V_s \leq \mu_{N+1}/e \leq V_d \tag{6}$$

The application of source-drain voltage V_{sd} of opposite sign means mathematically the reversing the inequality symbols in (6).

Simultaneously, it means physically that the electrons flow in the opposite direction, i.e., from the drain to source.

$\Longrightarrow$ In QD's, the notions of source and drain are a matter of convention only.

Therefore, we can speak about the first and second, left and right, upper and lower electrodes.

Tunnelling condition (5) consists of weak inequalities. This means that the electron can tunnel through the nanosystem even if $V_{sd} = 0$.

If tunnelling condition (5) is satisfied,number N of electrons in the QD changes as follows:

$$N \to N+1 \to N \to \ldots \tag{7}$$

This means that the single electron tunnels from the first electrode via QD, in which N excess electrons are confined, to the second electrode. In this case, we are speaking that the **transport window** opens up [cf. condition (6)].

If tunnelling condition (5) is not satisfied, the number of electrons in the QD remains constant

$$N = const\ .$$

In this case, we are dealing with **a quantum Coulomb blockade**, which results from a discreteness of energy spectrum of QD confined electrons.

Experiments show that for $N \leq\sim 20$ the electron energy levels are non-equidistant, i.e.,

$$\Delta E^N_{mn} \neq \Delta E^N_{m'n'}\ ,$$

which leads to unequally spaced tunnelling current peaks as a function of gate voltage. $\Longrightarrow$ **quantum Coulomb blockade**

If the number of electrons in the QD is large ($N \simeq 100$), the energy level spacings decrease and become equal to each other. In this case, the electron system exhibits classical properties: the separations between the tunnelling current peaks (on the gate voltage scale) become equal to each other. $\Longrightarrow$ **classical Coulomb blockade**

The classical Coulomb blockade results from the constant charging energy of the QD by the single electron.

According to the classical electrodynamics, the energy needed to add the single electron to the system of electrical capacitance C is equal to

$$\Delta E = \frac{e^2}{C}\ . \tag{8}$$

The corresponding difference of the gate voltage is

$$\Delta V_g = \frac{e}{C} = const \tag{9}$$

$\Longrightarrow$ equally spaced peaks of the source-drain current as a function of gate voltage

4.4 Experimental results

4.4.1 Single-electron capacitance spectroscopy

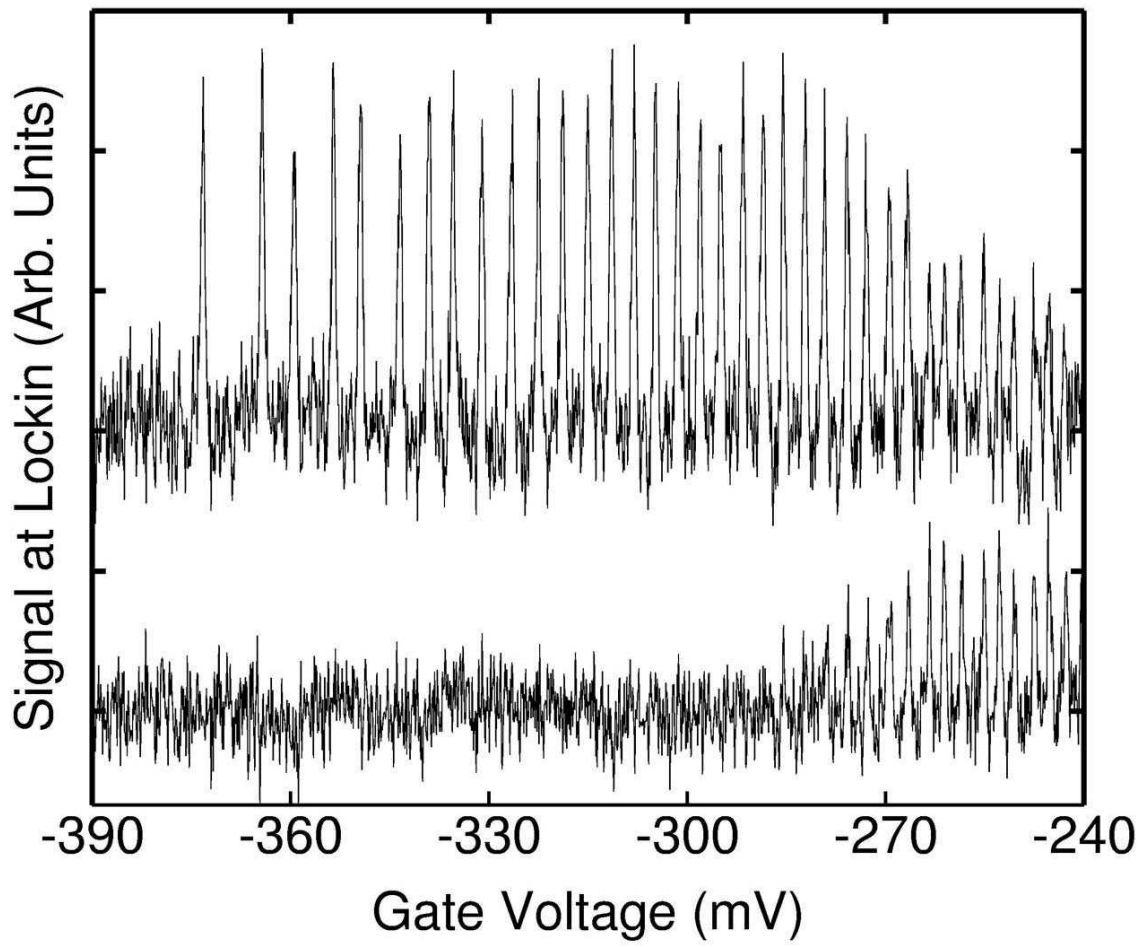

Figure 13: Capacitance of two-terminal QD [R.C. Ashoori et al., MIT] measured as a function of gate voltage. The first high peak on the left side corresponds to the first electron tunnelling to the dot.

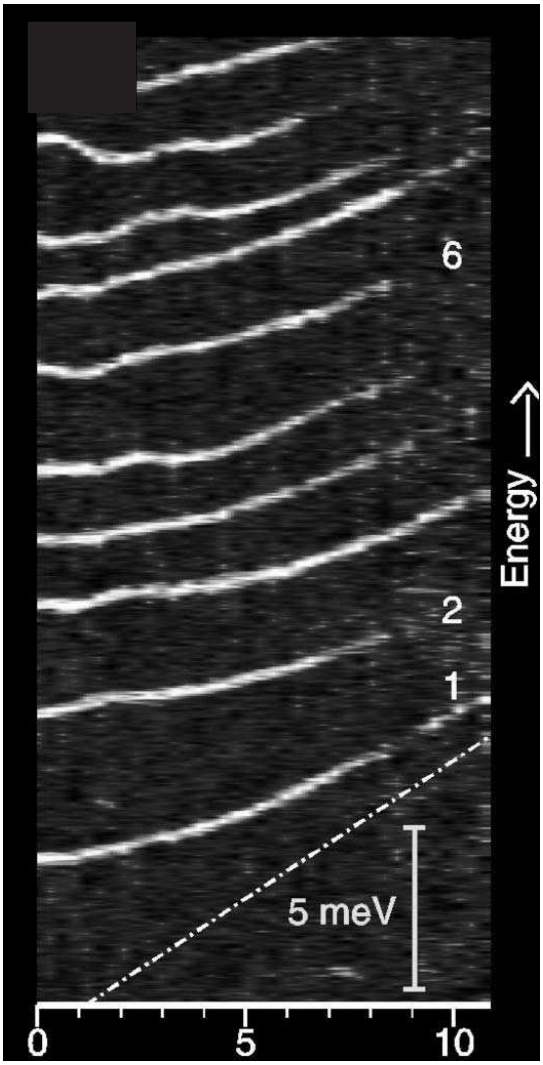

Figure 14: Results of capacitance measurements for two-terminal QD [R.C. Ashoori et al., MIT] for the first 10 electrons entering the dot as a function of magnetic field.

4.4.2 Single-electron transport spectroscopy

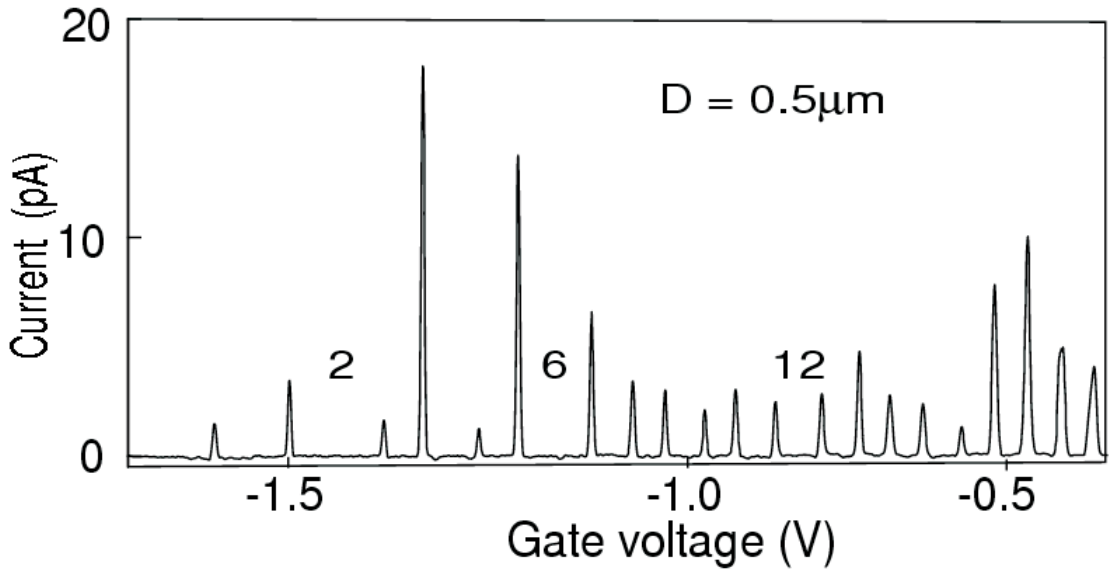

Figure 15: Source-drain current as a function of gate voltage at $V_{sd} = 150\mu$V for three-terminal QD [S. Tarucha et al., NTT].

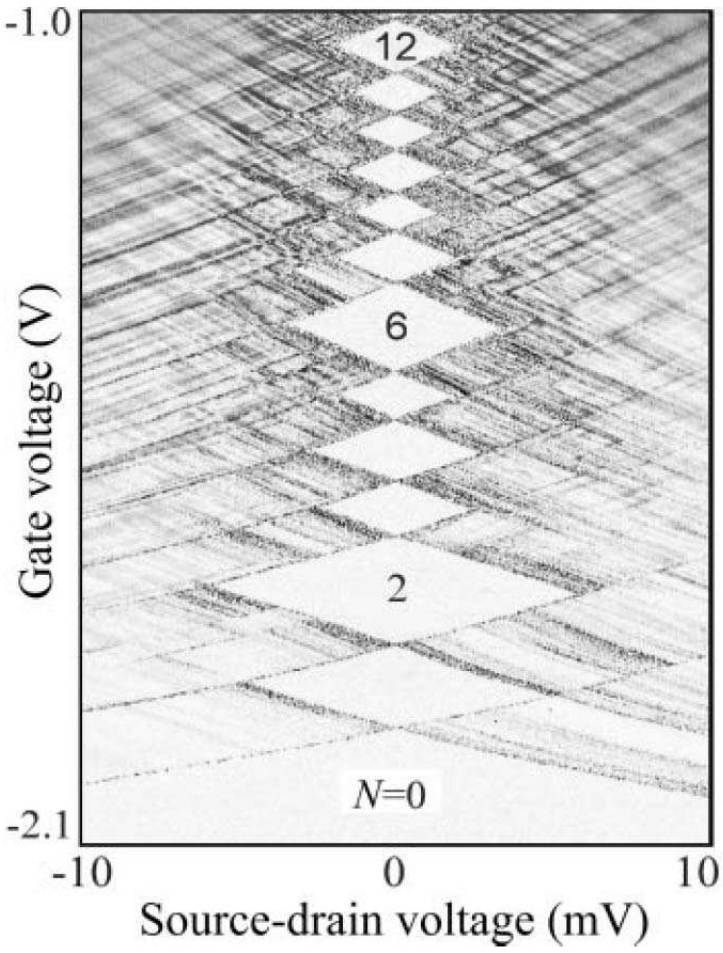

Figure 16: Differential conductance $\partial I/\partial V_{sd}$ (gray scale) on $V_g - V_{sd}$ plane for $B = 0$. In white rhombs (diamonds), $\partial I/\partial V_{sd} \simeq 0$ as a result of Coulomb blockade, and the number of electrons in the dot is fixed. [L.P. Kouwenhoven et al., TU Delft].

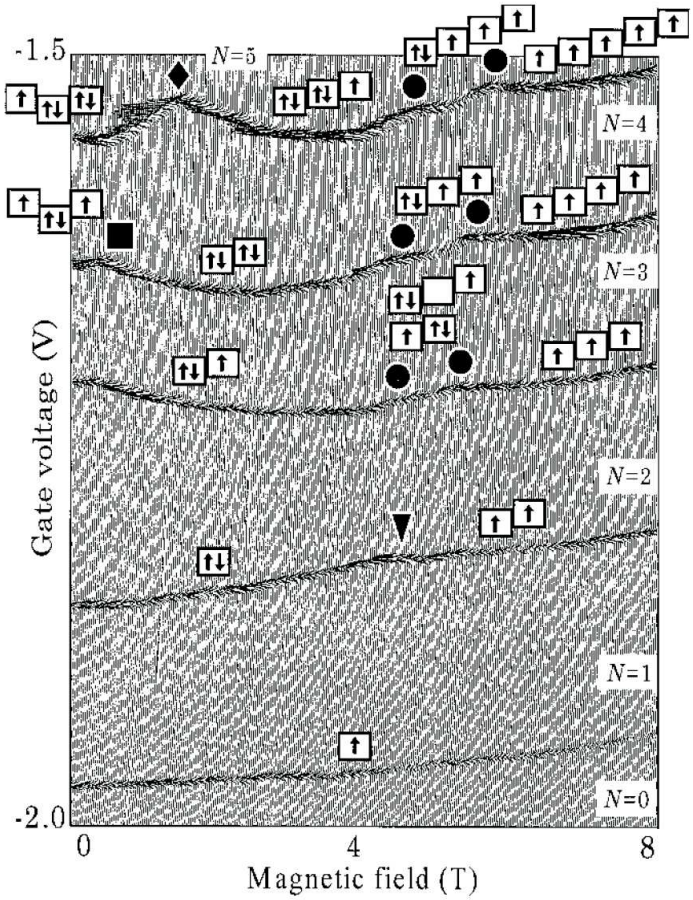

Figure 17: Source-drain current peaks as a function of gate voltage and magnetic field measured for $V_{sd} = 0.1$ mV. Arrows denote the spin state occupancy. Symbols (triangles, circles, etc.) correspond to phase transitions in the N-electron ground state. Number N of electrons is constant between each two curves as a result of Coulomb blockade [L.P. Kouwenhoven et al., TU Delft].

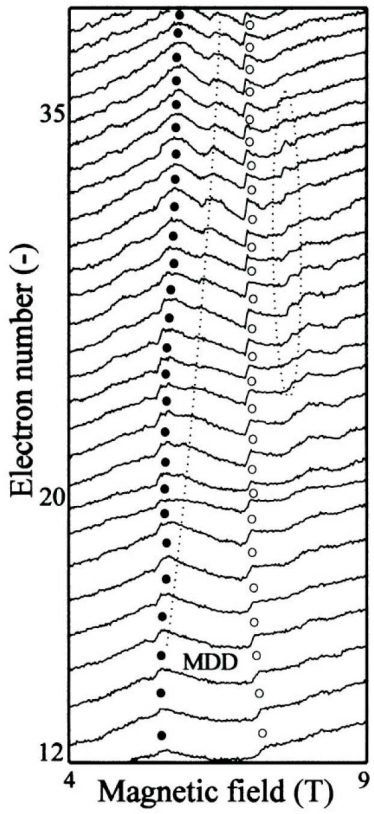

Figure 18: Gate voltage corresponding to source-drain current peaks for $V_{sd} =$ 0.1 mV as a function of magnetic field for different numbers of electrons listed at y axis. Full (empty) dots show the beginning (end) of Maximum Density Droplet (MDD) stability region. Dotted oval marks the region of rapid electron density changes in the QD [T.H. Oosterkamp et al., TU Delft].